Characterization of Single Actin-Myosin Interactions

Jeffrey T. Finer, Amit D. Mehta, and James A. Spudich
Departments of Biochemistry and Developmental Biology, Beckman Center, Stanford University Medical Center, Stanford, California 94305 USA

ABSTRACT The feedback-enhanced laser trap assay (Finer et al., 1994) allows the measurement of force and displacement produced by single myosin molecules interacting with an actin filament suspended in solution by two laser traps. The average displacement of 11 nm at low load and the average force of 4 pN near isometric conditions are consistent with the conventional swinging cross-bridge model of muscle contraction (Huxley, 1969). The durations of single actin-myosin interactions at low load, 3–7 ms, suggest a relatively small duty ratio. Event durations can be increased either by reducing the ATP concentration until ATP binding is rate-limiting or by lowering the temperature. For sufficiently long interactions near isometric conditions, low frequency force fluctuations were observed within the time frame of a single event. Single myosin events can be measured at ionic strengths that disrupt weak binding actomyosin interactions, supporting the postulate of distinct weak and strong binding states. Myosin-generated force and displacement were measured simultaneously against several different loads to generate a force-displacement curve. The linear appearance of this curve suggests that the myosin powerstroke is driven by the release of a strained linear elastic element with a stiffness of approximately 0.4 pN nm^{-1}.

INTRODUCTION

During the past few years, major advances in the development of in vitro assays for molecular motor function have culminated in the first direct measurements of forces and displacements produced by single molecules (Kuo and Sheetz, 1993; Svoboda et al., 1993; Finer et al., 1994; Hunt et al., 1994; Ishijima et al., 1994; Miyata et al., 1994). The major technological advances have come in the development of mechanical probes, namely, laser traps (optical tweezers) and glass microneedles. When combined with high resolution detection systems, these probes can provide quantitative measurements of nanometer displacements and piconewton forces on millisecond time scales. These detection limits are well matched to the mechanical properties of the molecular motor proteins myosin and kinesin.

Single myosin forces and displacements have been recorded recently using a feedback-enhanced laser trap assay (Finer et al., 1994). A single actin filament held by two laser traps via beads attached near each end is maneuvered into close proximity of a coverslip-bound silica bead decorated with heavy meromyosin (HMM) molecules (Fig. 1). Sensitive silicon photodetectors are used to monitor nanometer displacements of the trapped bead with millisecond resolution. Discrete stepwise displacements of actin produced by single myosin molecules were observed under low load conditions, and discrete myosin force transients were measured near isometric conditions. The average unitary displacement of 11 nm and unitary force of 3–4 pN are consistent with predictions of the conventional swinging cross-bridge model of muscle contraction (Huxley, 1969).

In the present work, we describe several extensions of this assay that allow additional characterization of the mechanical properties of a myosin powerstroke. Single actin-myosin interactions can be prolonged either by reducing the ATP concentration or by lowering the temperature. Thus, the optical trap assay serves as a tool for kinetic measurements at the single molecule level. Once event durations become sufficiently long, Fourier analysis can be used to examine the spectral features of force or displacement fluctuations in the course of a single actin-myosin interaction. Additionally, the assay can be used to test myosin function under experimental conditions that affect a particular type of intermolecular interaction. For instance, changes in ionic strength will affect the electrostatic interactions involved in the initial weak binding state between actin and myosin. Finally, by varying feedback parameters, trap stiffness can be adjusted and myosin force and displacement can be measured over a range of elastic loads. Thus, myosin-induced force can be measured as a function of partial displacement.

MATERIALS AND METHODS

Feedback-enhanced laser trap

The feedback-enhanced laser trap system (Fig. 2) as described (Finer et al., 1994) uses a diode-pumped Nd:YLF laser (Spectra-Physics, Mountain View, CA, TFR; 1.047 μm). The laser light is split by polarizing beamsplitters to form two trapping beams (second beam not shown in Fig. 2), which are focused through a high numerical aperture objective (Zeiss, 63X Planapochromat, 1.4 NA, DIC grade) onto the stage of a custom-built, inverted microscope. The trap positions can be adjusted using motorized mirrors to steer the laser beam slowly or using electronically controlled acousto-optic modulators to deflect the beam rapidly. Brightfield illumination with a xenon arc lamp is used to project the image of a trapped bead onto a quadrant photodetector, and high resolution position measurements are derived from the differential current outputs of the photodiode elements. The effective stiffness of one optical trap can be greatly enhanced by means of a negative feedback circuit that uses the bead position signal, after processing with proportional and integral gain, to drive the acousto-optic modulators.

Address reprint requests to Dr. Jeffrey T. Finer, Department of Biochemistry, Beckman Center, Stanford University Medical Center, Stanford, CA 94305. Tel.: 415-725-6376; Fax: 415-725-2929; E-mail: finer@cmgm.stanford.edu.

0006-3495/95/04/291s/07 $2.00

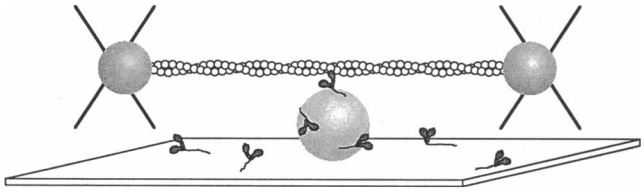

FIGURE 1 Schematic diagram of the single actin-myosin interaction assay. A single actin filament with polystyrene beads attached near each end is held in mid-solution by two laser traps. The filament is pulled taut and held near a single HMM molecule on the surface of a silica bead that is attached to a microscope coverglass. The actin-myosin interaction is then monitored by projecting an image of one of the trapped beads onto a quadrant photodiode detector (not shown) for high resolution position measurements.

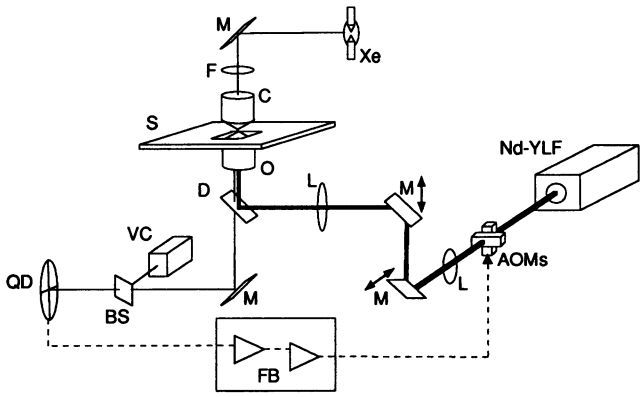

FIGURE 2 Schematic diagram of the feedback-enhanced laser trap system. The thick solid line represents the laser beam path; the thin solid line represents the imaging path. Brightfield illumination from a xenon arc lamp (Xe) is used for visualizing the sample with a video camera (VC) and used to project an image of a trapped bead in the specimen plane (S) onto a quadrant photodetector (QD). Two orthogonal acousto-optic modulators (AOMs) are used for rapidly deflecting the laser beam before it enters the back aperture of the microscope objective (O). Additional optics include lenses (L), mirrors (M), dichroic filter (D), interference filter (F), beamsplitter (BS), and microscope condenser (C). The second trapping beam and fluorescence imaging pathways are not shown for simplicity. The quadrant detector output (- - - -) may be processed by feedback electronics (FB) and used to drive the acousto-optic modulators.

Fine control of trap stiffness is achieved either by altering the laser power (Simmons et al., 1995) or by adjusting the gain parameters in the feedback circuit.

Position signals are calibrated by using the acousto-optic modulators to produce fixed displacements of a trapped bead and monitoring the corresponding signal outputs from the quadrant detector. For beads 1 μm in diameter, the quadrant detector output varies linearly with bead position for displacements of up to approximately 200 nm away from the center of the detector. The trap stiffness is calibrated by applying viscous forces to a trapped bead by solution flow produced by moving a microscope substage with piezoelectric transducers (Finer et al., 1994). The bead displacement is proportional to the applied force for displacements of up to 300 nm away from the trap center. Therefore, the distance between the center of the bead and the center of the trap can be used to measure externally applied forces. When the feedback loop is closed, the laser beam moves to suppress bead motion, and both the bead position and the trap position are necessary to calculate the applied force.

Single myosin motor assays

Silica beads (1-μm diameter) were attached to a microscope coverslip, which was then coated with nitrocellulose and used to construct a flow cell as described previously (Finer et al., 1994). The coverslip surface was then decorated with rabbit skeletal muscle HMM at a density that was insufficient to support continuous movement of actin filaments in a sliding filament assay. Polystyrene beads with *N*-ethylmaleimide (NEM)-treated HMM covalently linked were mixed with rhodamine-phalloidin-labeled actin filaments and introduced into the flow cell in motility buffer (25 mM KCl, 4 mM $MgCl_2$, 1 mM EGTA, 10 mM DTT, 25 mM imidazole, 2 mM ATP, pH 7.4). Two trapped beads were placed near the ends of a single actin filament that was visualized by epifluorescence, and the beads were separated until essentially all compliance in the actin-bead system was removed. The actin filament was then brought into the vicinity of a silica bead on the surface. With sufficiently low surface HMM density, discrete displacements of one of the trapped beads could be observed in the direction parallel to the long axis of the actin filament. When the feedback loop was closed, discrete changes in the trap position, representing force transients, could be observed along the same axis.

The durations of single interactions could be increased by limiting ATP concentrations (1–10 μM) in the motility buffer. In these cases, the ATP concentration was maintained by including 1 mM phosphocreatine and 0.1 mg ml^{-1} creatine phosphokinase in the buffer. For high ionic strength measurements, 150 mM KCl was used in the motility buffer.

Data collection and analysis

The position of the trapped bead was monitored in the two dimensions of the image plane using a quadrant photodiode detector (bandwidth 100 Hz, single pole). Detector output signals were sampled at 4 kHz with an analog-to-digital converter (R. C. Electronics, Goleta, CA, ISC-16), and the resulting discrete time data were stored on a computer. When the feedback circuit was engaged and the gain parameters were optimized, the system bandwidth was increased to 830 Hz. Feedback signals driving the acousto-optic modulators have been shown to vary linearly with trap position and were calibrated as described previously (Simmons et al., 1995). Force measurements were derived by multiplying the difference between the trap and bead positions by the measured trap stiffness.

Single myosin events were scored according to the following criteria. The baseline level of background Brownian motion before and after the event were required to be identical. The displacement or force transient had to have a sharp, rapid transition to and from a plateau above the baseline Brownian motion. Finally, each scored event was required to be clearly distinct and temporally isolated from other fluctuations above baseline. When event durations were long relative to those at the bandwidth limit, additional digital filtering (200 Hz, eighth-order Butterworth lowpass, zero phase distortion) was used to decrease the threshold level for distinguishing events from the background Brownian motion. When event durations were near the bandwidth limit, amplitude and duration were measured without digital filtering.

Significantly prolonged events at 1 μM ATP were analyzed to determine the frequency content at the peak compared with that of the baseline. In each case, a power spectrum of the event plateau was compared with the power spectrum of an equal amount of baseline data. Independent spectra were taken of 1000 point windows (0.25 s) from several events and then averaged point-by-point to ensure that the frequency content remained constant throughout a given event and among different ones. Both the event plateau and the baseline spectra were normalized by the same constant to facilitate amplitude comparison between the two.

RESULTS AND DISCUSSION

Single myosin mechanics

When a single actin filament held by two laser traps via attached polystyrene beads is brought into the vicinity of a

surface silica bead coated sparsely with HMM, discrete displacements are seen in the direction parallel to the long axis of the filament (Fig. 3). In contrast, very little motion is seen in the perpendicular direction (data not shown). The single displacements range from 7 to 17 nm with a mean value of approximately 11 nm (Finer et al., 1994). The peak value is not significantly different for trap stiffnesses ranging from 0.02 to 0.11 pN nm^{-1} that allow myosin movement against relatively low load. Increased stiffness suppresses thermally driven Brownian motion and enhances the signal-to-noise ratio, thereby decreasing the threshold for event detection; however, as stiffness continues to increase, displacement amplitudes can be reduced significantly (see below). At saturating ATP concentration (2 mM), the durations of single displacements are 6.4 ± 3.6 ms (mean ± SD; $n = 41$). These durations are at the lower limit of those detectable with a detector bandwidth of 100 Hz and, therefore, are likely to reflect an upper limit for the duration of a single myosin displacement at low load. The detector bandwidth, however, does not allow us to place a lower limit on the duration.

Single force transients can be measured under the same conditions by simply engaging the feedback circuit, thus increasing effective trap stiffness approximately 300-fold to allow measurements near isometric conditions. At a trap stiffness of 6 pN nm^{-1}, single force transients ranging from 1 to 7 pN, with an average value of approximately 4 pN were measured (Finer et al., 1994). For single force transients, the signal-to-noise ratio is increased as the trap stiffness is decreased. However, if the trap is too compliant, the feedback system may respond to a myosin-induced force by moving the trap outside the range where the trap stiffness is linear. Thus, a practical lower limit exists for the trap stiffness. For a given interaction between a single actin filament and an HMM-coated surface bead, single displacements and single force events occur at approximately the same frequency.

We are thus able to measure the displacement and force produced by single myosin molecules on single actin filaments. A few limitations remain, however, and are reflected in the data. The broad distribution of single event amplitudes most likely represents the random orientation of HMM molecules on the surface relative to the actin filament fixed in solution. The durations of single events are limited at the low end by the bandwidth of the detector; however, we can place an upper limit on the single event duration and, hence, the myosin duty ratio (Finer et al., 1994).

Single myosin kinetics

The durations of single myosin displacements and force transients can be increased by decreasing the ATP concentration to delay the dissociation of myosin from actin. For ATP concentrations well below the K_m for ATP in a sliding filament assay (50 μM) (Kron and Spudich, 1986), the average single displacement and force durations show sensitive dependence upon the ATP concentration (Finer et al., 1994). As a result, we are able to calculate the second-order rate constant for ATP binding from the average duration of single displacements at 1 μM ATP. The value of 3.8 ± 0.4 $M^{-1}\,s^{-1}$ agrees well with the rate constant for the acto-S1 ATPase measured in solution (White and Taylor, 1976). The increase in duration of the actin-myosin interaction at limiting ATP concentrations indicates that ATP binding and, hence, the completion of the ATP hydrolysis cycle, is required for each interaction. For a given limiting ATP concentration, there is a wide variation in the duration of individual actin-myosin interactions. This is illustrated by the distribution of HMM displacement durations shown in Fig. 4. The probability of a given event duration declines exponentially as the duration increases. This is analogous to the distribution of open times for single ion channels (Sakmann and Neher, 1983) and indicates that a first-order kinetic process limits the rate of myosin detachment.

An alternate approach to slowing the dissociation of myosin from actin is to decrease the temperature. At saturating ATP concentration (2 mM), the mean event duration for single displacements was 15 ± 20 (mean ± SD; $n = 44$) at 17°C compared with 6.4 ± 3.6 ms (mean ± SD; $n = 41$) at 25°C. The difference is significant and consistent with previously observed decreases in sliding filament velocity in vitro (Homsher et al., 1992) and decreases in the rates of post-stroke product release measured in solution for a similar

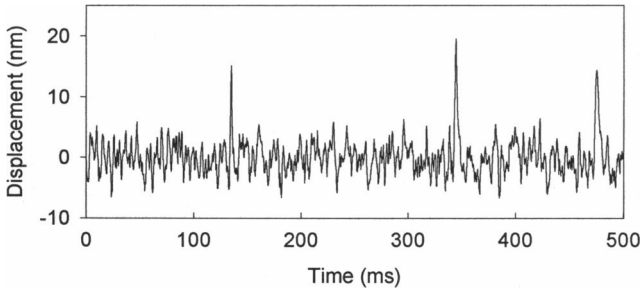

FIGURE 3 Single HMM displacements at saturating ATP concentration (2 mM). The data trace shows the movement of the trapped bead in the direction along the actin filament. Trap stiffness, 0.12 pN nm^{-1}.

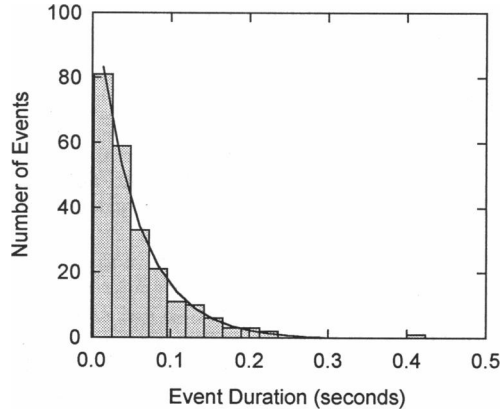

FIGURE 4 Distribution of single HMM displacement durations. The curve is a single exponential fit to the distribution of durations. ATP concentration, 10 μM. Trap stiffness, 0.42 pN nm^{-1}.

decrease in temperature (White and Taylor, 1976). If a first-order kinetic process is rate-limiting, we again expect an exponential distribution of durations that may give rise to a SD greater than the mean as seen at 17°C. The displacement durations at 25°C are again likely to be bandwidth-limited, which would account for the smaller SD.

Single myosin event analysis

Single myosin displacements and force transients reach plateau levels above the baseline Brownian motion during the time when myosin is bound to actin. The duration of the plateau can be increased by reducing the ATP concentration as described above. Fourier analysis was used to compare the spectral pattern of the fluctuations at the plateau of a single myosin event with that of the baseline Brownian motion between interactions. Analysis of position noise in the plateau of a prolonged displacement event showed a decrease in amplitude relative to the background level throughout the examined bandwidth (Fig. 5 *A–C*). In contrast, when prolonged, single force events were analyzed, fluctuation amplitude increased relative to baseline below approximately 200 Hz and decreased slightly at higher frequencies (Fig. 5 *D–F*).

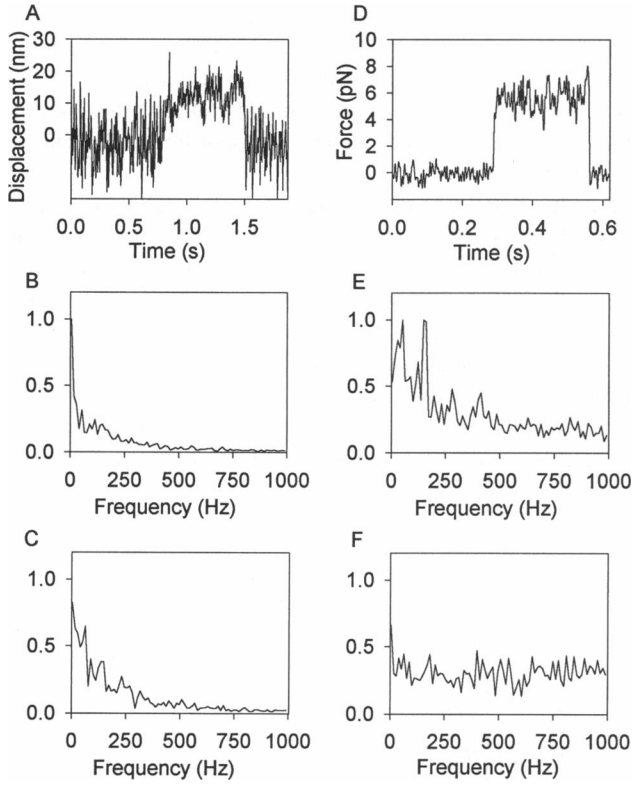

FIGURE 5 (*A*) Single HMM displacement event at 1 μM ATP. Lowpass filtering demonstrates a reduction in low frequency noise at the displacement plateau relative to the baseline. (*B* and *C*) Power spectra of the signal segment at the displacement plateau (*B*) and the baseline signal (*C*). Both displacement spectra are normalized by the same constant to facilitate comparison. (*D*) Single HMM force event at 1 μM ATP. Lowpass filtering demonstrates an increase in low frequency noise at the force plateau relative to the baseline. (*E* and *F*) Power spectra of the signal segment at the force plateau (*E*) and the baseline signal (*F*). Both force spectra are normalized by the same constant to facilitate comparison.

Control experiments were performed (data not shown) to test whether the changes in force and position fluctuations at event plateaus were dependent upon myosin. To simulate a constant force, a steady viscous force, equal in magnitude to the average myosin force transient, was applied to a free trapped bead. The force and position signals appeared very similar to those of the baseline Brownian motion and unlike the single myosin event plateaus in both the time and frequency domains. To test the contribution of an actin filament under stress to the fluctuation, a tension of approximately 2.5 pN was applied to a trapped actin filament by slowly separating the two trapped beads. In this case, the position and force fluctuations exhibited mild, broadband reduction relative to those of a free bead. This is most likely due to the additional constraint on bead motion provided by the actin filament and the second optical trap. The broadband noise reduction, however, is less than that seen for single myosin displacements and does not exhibit the increase in low frequency fluctuations observed with single force transients. The changes in fluctuations at the event plateaus thus seems to be dependent on myosin bound to the actin filament.

The most likely explanation for the reduction in noise amplitude at the plateau of a single myosin displacement is the stiffness of the actin-myosin rigor linkage. The rigor linkage would provide an additional passive constraint on bead motion and, thus, should suppress the amplitude of the thermally induced Brownian motion at all frequencies. The increased low frequency noise at the plateaus of single force events, however, could not be explained by the simple addition of a passive constraint. Thus, the actin-myosin complex near isometric conditions is not likely to represent a simple rigor linkage. Because the system containing the trapped beads, taut actin filament, and bound myosin is overdamped, and the low frequency noise appears to continue throughout long events, the noise is also unlikely to reflect oscillation about a potential energy minimum. Rather, the myosin-induced force is likely to be fluctuating in a single pre-rigor interaction.

Ionic strength effects on single myosin events

The laser trap assay can also be used to examine actin-myosin interactions under solution conditions that disrupt a particular type of intermolecular force. To investigate the role of electrostatic binding in movement driven by single and multiple myosin molecules, the optical trap assay and the conventional sliding filament assay were conducted at low and high ionic strength. Both sliding filaments and single molecular forces and displacements were observed when the motility buffer included 25 mM KCl. When the KCl concentration was increased to 150 mM, actin filaments diffused away from the myosin-decorated surface in the sliding filament assay. In contrast, using the optical trap assay, unitary displacements and forces could be observed under these

conditions. Event amplitudes and durations were unchanged by the increase in ionic strength.

These observations support the hypothesis that electrostatic, weak-binding interactions contribute to holding actin filaments near the surface in the sliding filament assay. Such interactions by myosin heads, which are not actively contributing to movement or force production, are disrupted by increases in ionic strength, and filaments easily diffuse away from the surface. In the laser trap assay, however, the two traps can be used to hold an actin filament in close proximity to a surface bound myosin head, thus bypassing the need for weak-binding interactions for motility to be observed. Additionally, the measurement of consistent event amplitudes and durations at low and high ionic strength suggests that the strong binding states involve other types of binding, such as hydrophobic interactions.

Single myosin force-displacement curve

In previous work, the feedback-enhanced laser trap assay (Finer et al., 1994) was used to measure single myosin displacements at low load and single myosin force transients near isometric conditions. Glass microneedles (Ishijima et al., 1994) were used to measure interactions at intermediate stiffnesses, and it has been shown that it is possible to construct a force-displacement curve by measuring single myosin events over a range of stiffnesses. To characterize the change in myosin's force as it progresses through an entire powerstroke, single force and displacement transients were measured against several loads spanning the range of stiffness from low load (0.02 pN nm^{-1}) to near-isometric conditions (4.1 pN nm^{-1}). In each case, the effective trap stiffness was set by adjusting the proportional gain in the feedback circuit to limit the trap response to bead motion. Each effective trap stiffness thus constrained the ratio of myosin-driven force to displacement. In this situation, myosin can move the trapped actin filament until the force it exerts is matched by the feedback-enhanced optical load on the trapped bead. An example data trace (Fig. 6 *A*) shows myosin moving and exerting force against a 0.5 pN nm^{-1} trap load. A curve of force versus displacement was generated by plotting the mean amplitude of myosin force against the corresponding displacement for several trap stiffnesses. At each stiffness setting, event amplitudes were broadly distributed, which again may be due to the random relative orientations of the HMM molecules and the actin filament. If either the mean values or the higher ends of the amplitude distributions are used, the force appears to vary linearly with displacement (Fig. 6 *B*).

The linear appearance of the force-displacement curve suggests that the release of a strained elastic element is the driving force in the myosin powerstroke. The stiffness of the elastic element would be equal to the slope of the force-displacement curve, approximately 0.4 pN nm^{-1}. Additionally, if the force measured against various elastic loads is interpreted to be the force exerted by myosin after it has moved by the corresponding distance to an intermediate state

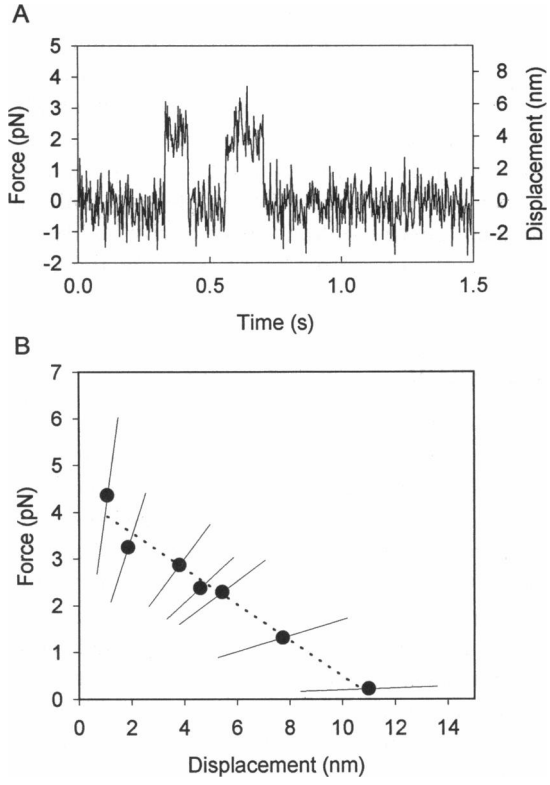

FIGURE 6 (*A*) Single HMM events at an intermediate trap stiffness (0.52 pN nm^{-1}). ATP concentration, 10 μM. (*B*) Force versus displacement for single HMM molecules. Each data point represents the mean force and displacement produced by single HMM molecules at a given trap stiffness (n = 30–100). For each point, the error bar indicates the range for data within 1 SD of the mean. The trap stiffness is indicated by the slope of the error bar in each case. A linear fit through the data is indicated by the dashed line.

within a normal powerstroke, the area under the force-displacement curve represents the mechanical work done during a powerstroke. If the mean event amplitudes are used for each stiffness, the area under the curve is approximately 24 pN · nm (2.4×10^{-20} J), and if the higher end of each distribution is used, the area is approximately 42 pN · nm (4.2×10^{-20} J). To calculate myosin's thermodynamic efficiency, it is necessary to estimate the input energy from ATP hydrolysis. For the conditions within a muscle cell, the available energy from ATP hydrolysis is 10^{-19} J (Bagshaw, 1993). Therefore, the efficiency of a myosin powerstroke in using the energy from ATP hydrolysis is 24–42%. These values must be interpreted with caution because the energetics of ATP binding and product release are not accounted for. Nevertheless, the high average efficiency of the myosin motor as an energy transducer would be consistent with models of tight coupling between myosin's ATP hydrolysis cycle and its mechanical cycle.

The linear force-displacement curve can be compared with the portion of the T2 tension recovery profile corresponding to quick release experiments on contracting muscle fibers (Huxley and Simmons, 1971). Unlike the curve discussed here, the T2 contour is significantly nonlinear and is concave

downward. One possible explanation for this inconsistency is the difference in the periodicity of thick and thin filaments, which would result in a distribution of cross-bridge angles with respect to the filament axis. If several linear, elastic cross-bridges were strained by different amounts, a nonlinear tension recovery might be expected after a quick release. Therefore, the single molecule force-displacement curve would not necessarily be identical to that for multiple interactions constrained by the geometry of a muscle fiber.

CONCLUSIONS

tk;2Here we have described a few extensions of the feedback-enhanced laser trap assay for myosin function, which allow further characterization of single actin-myosin interactions. In addition to simple force and displacement measurements, we are able to study kinetics at the molecular level, the effects of electrostatic interactions, force fluctuations within a single interaction, and myosin's force-displacement curve. These assays, each individually contributing to our understanding of myosin's mechanochemical energy transduction, represent just a sample of the many extensions of the single myosin assay to be seen in the next few years.

This work was supported by grants from National Institutes of Health and the Human Frontier Science Program (J. A. Spudich). J. T. Finer is a trainee of the Medical Scientist Training Program at Stanford University School of Medicine. A. D. Mehta is a trainee of the Biophysics Program at Stanford University.

REFERENCES

Bagshaw, C. R. 1993. Muscle Contraction. Chapman & Hall, London.

Finer, J. T., R. M. Simmons, and J. A. Spudich. 1994. Single myosin molecule mechanics: piconewton forces and nanometre steps. *Nature.* 368: 113–119.

Homsher, E., F. Wang, and J. R. Sellers. 1992. Factors affecting movement of F-actin filaments propelled by skeletal muscle heavy meromyosin. *Am. J. Physiol.* 262:C714–C723.

Hunt, A. J., G. Gittes, and J. Howard. 1994. The force exerted by a single kinesin molecule against a viscous load. *Biophys. J.* 67:766–781.

Huxley, A. F., and R. M. Simmons. 1971. Proposed mechanism of force generation in striated muscle. *Nature.* 233:533–538.

Huxley, H. E. 1969. The mechanism of muscular contraction. *Science.* 164: 1356–1366.

Ishijima, A., Y. Harada, H. Kojima, T. Funatsu, H. Higuchi, and T. Yanagida. 1994. Single molecule analysis of the actomyosin motor using nano-manipulation. *Biochem. Biophys. Res. Commun.* 199:1057–1063.

Kron, S. J., and J. A. Spudich. 1986. Fluorescent actin filaments move on myosin fixed to a glass surface. *Proc. Natl. Acad. Sci. USA.* 83: 6272–6276.

Kuo, S. C., and M. P. Sheetz. 1993. Force of single kinesin molecules measured with optical tweezers. *Science.* 260:232–234.

Miyata, H., H. Hakozaki, H. Yoshikawa, N. Suzuki, K. Kinosita, T. Nishizaka, and S. Ishiwata. 1994. Stepwise motion of an actin filament over a small number of heavy meromyosin molecules is revealed in an in vitro motility assay. *J. Biochem.* 115:644–647.

Sakmann, B., and E. Neher. 1983. Single-Channel Recording. Plenum Press, New York.

Simmons, R. M., J. T. Finer, S. Chu, and J. A. Spudich. 1995. Quantitative measurements of force and displacement using an optical trap. *Biophys. J.* In press.

Svoboda, K., C. F. Schmidt, B. J. Schnapp, and S. M. Block. 1993. Direct observation of kinesin stepping by optical trapping interferometry. *Nature.* 365:721–727.

White, H. D., and E. W. Taylor. 1976. Energetics and mechanism of actomyosin adenosine triphosphatase. *Biochemistry.* 15:5818–5826.

DISCUSSION

Session Chairperson: Kenneth A. Johnson
Scribe: Alexander L. Friedman

LOMBARDI: Can you go back to the record that you show in isometric conditions? I mean the force step. The force step at low ATP. Did you do statistics on this? Is this a continuous distribution, or is there a concentration at two levels of force?

FINER: We did do statistics on this, and it forms a very broad distribution. It doesn't break up into two levels at all.

KINOSITA: This is a question to you as well as ourselves. Frankly, I do not understand in our case why we can see steps and in your case too. If there is any compliance between your myosin and the glass surface, you should not be able to see the steps. The fact that you have been able to see the steps with 5pN, or something like that, implies that there is virtually no compliance between your myosin and the glass surface. Have you somehow measured that?

FINER: We haven't measured that compliance specifically. You guys measured it, right?

KINOSITA: This partially answers Jerry Pollack's question. One possibility in our case, possibly in your case too, is that the myosin also does the hand-over-hand movement. In this case, one myosin can hold it and stretch the self-compliance, while the other one is making force. This is one possibility, but otherwise I cannot understand why we see steps and why you see steps.

FINER: Yes. I guess in our case we have to assume that the proteins are well bound to the surface, that there isn't a compliant element between the protein and the surface, but any sort of compliant element within the protein, I don't think, would influence whether or not we would see these events.

BLOCK: This is the counterpart of what Kinosita is saying. Not only must there not be any series compliance, or very little of it associated with the HMM, but the HMM is bound on a support, namely, this glass bead you have down on this coverslip, and that's not allowed to rock.

FINER: That's right. We have done studies of that motion.